11-16-2017

Non-Orthogonal Multiple Access in a mmWave Based IoT Wireless System with SWIPT

Haijian Sun
Utah State University, haijian.sun@aggiemail.usu.edu

Qun Wang
Utah State University, claudqunwang@gmail.com

Shakil Ahmed
Utah State University, shakil.ahmed@aggiemail.usu.edu

Rose Qingyang Hu
Utah State University, rose.hu@usu.edu

Non-Orthogonal Multiple Access in a mmWave Based IoT Wireless System with SWIPT

(Invited Paper)

Haijian Sun, Qun Wang, Shakil Ahmed, Rose Qingyang Hu
Department of Electrical and Computer Engineering
Utah State University, Logan, UT, USA
Emails: {h.j.sun, claudqunwang, shakilahmed, rosehu}@ieee.org

***Abstract*—This paper applies non-orthogonal multiple access (NOMA) and relaying schemes in a mmWave based wireless heterogeneous system that aims to support Internet of Things (IoT) applications. The system consists of high power base stations, low-power relays, and low-power IoT devices. Due to the ad hoc deployment nature of low-power relays, they have very limited access to wireline power charging facilities. Furthermore, IoT devices normally have limited power and short battery life. The study assumes low-power relays and IoT devices are capable of energy harvest functionality. With the help of relays or IoT devices, downlink NOMA transmission consists of two phases. In the first phase, the BS sends a composite signal to a UE and a selected relay simultaneously by applying NOMA. After receiving the signal, relay or the IoT device split the signal into two parts. One part is for information decoding and the other part is for energy harvesting. In the second phase, the BS sends another message to UE 1 while the relay sends the decoded message to UE 2 by using the harvested energy in phase 1. The outage problem of the proposed scheme is analyzed and simulations results are presented to verify the theoretical results.**

***Keywords*—D2D, Heterogeneous network, IoT, NOMA, Relay, Outage probability, SWIPT**

I. Introduction

The unprecedented growth of mobile devices including smart phones, tablets, laptops, and IoT devices drives the wireless telecommunication industry to a new level. The requirements come from various aspects such as higher data rate, fairness, tremendous connectivity, and low latency from different applications and various end users. Therefore, as a new generation technology, 5G emerges with its goal to provide 1000 times higher data rate, 1 ms low latency, and support billions of upcoming Internet of things (IoT) devices. Among these features, 1000 times capacity can be achieved by the new millimeter wave (mmWave) spectrum, novel network architectures and new radio access technologies (RATs) [1].

Wireless heterogeneous network with a combination of macro base stations (MBSs) and small BSs such as femto nodes, pico nodes and relays can not only provide high data rate to cell center users but also extend coverage to cell edge users[1]. Emerging new RATs can help support more users and provide higher system capacity. Among those RATs, power domain non-orthogonal multiple access (NOMA) attracts great research interests both in industry and academia recently. The main principle of NOMA is to assign different transmit powers to mulitple users and allow these users to share the same physical resources for transmission. At the receiver side, advanced receiver technology such as successive interference cancellation (SIC) is applied to decode multiple signals sequentially. SIC first decodes the signal that has the highest signal-to-interference-noise ratio (SINR) and the decoded part is subtracted from the superimposed signal by estimating current channel information and reconstructing the modulated symbols. Compared with the conventional orthogonal multiple access (OMA) such as orthogonal frequency division multiplexing (OFDM) in 4G, the advantages of NOMA come from two-fold. First NOMA can support multiple users on the the physical resource and thus the overall spectral efficiency is improved. Second, NOMA can greatly increase system connectivity capability [2][3].

In [4], the authors present a NOMA performance analysis on outage probability with randomly deployed users. A closed-form formula is derived and they conclude that NOMA achieves a better performance compared with OMA techniques. A more fundamental result is illustrated in [5], which provides a theoretical study from information theory perspective. It concludes that NOMA, as a special case of superposition code, can achieve performance close to the Shannon limit. Furthermore, a great channel difference can benefit the system performance, which can be a general rule to form NOMA users.

Due to the ad hoc deployment nature of most low-power nodes and devices, they may have limited access to wireline power charging facilities and also have limited battery life. In this paper, low-power relay nodes and devices are assumed to be capable of energy harvest functionality. More specifically, simultaneous wireless information and power transfer (SWIPT) is considered. SWIPT can have two implementation modes, namely time switching (TS) mode and power splitting (PS) mode[6]. In the TS mode, a dedicated resource is used for energy transfer from which the harvested energy is then used for future information transmission. In the PS mode, upon receiving the radio signal, the energy harvest node splits the signal into two parts. The first part is used for signal decoding while the second part is used for energy charging. A linear energy harvest model, which assumes the output power of the energy harvest circuit grows linearly with the input power, is applied in most existing works. Cooperative NOMA system with SWIPT is studied in [7], where they proposed different user selection schemes and evaluate the performance with outage probability. This paradigm is proved impractical based

978-1-5090-5932-4/17/$31.00 ©2017 IEEE

on field test results as shown in [8]. As a result, a more practical yet more complicated non-linear model which better matches current circuit design is considered in this paper. Thus the wireless heterogeneous system in this study consists of higher power MBSs and low-power relays with SWIPT that is based on the non-linear energy harvesting model. Downlink NOMA is first used to transmit composite signals to UE and relay. Relay then harvests the energy by using non-linear model in PS mode. With the harvested energy, relay sends the received signal to the cell edge UE.

The rest of this paper is organized as follows. Section II introduces the system model. The outage probability analysis is presented in Section III. Numerical performance results are provided in Section IV. The paper is concluded in Section V.

II. System Model

The system model is based on a mmWave downlink wireless heterogeneous system that consists of high power MBSs, low-power relays, and low-power IoT devices, such as sensors or wearable devices. At mmwave band, MBSs are equipped with a large number of horn antennas, which have narrow half-power-beamwidth (HPBW) to combat with the severe pathloss and each transmission is conducted with a single antenna. While each low-power relay or IoT device is equipped with a single antenna due to the size and power constraints. It is assumed that MBSs can coordinate the transmission direction with a stepper motor, hence inter-cell and intra cell interference can be eliminated by carefully aligning the beam directions. Furthermore, relaying and NOMA are used to help reach UEs out of coverage due to severe blockage at mmWave band. Without loss of generality, IoT UE 1 and IoT UE 2 are selected, where UE 1 is in the beamforming coverage area while there is a severe blockage between BS and UE2 so that a direct transmission link between the MBS and UE 2 is difficult to establish. Thus BS can communicating to UE 2 through relays. In this paper we assume device to device (D2D) relaying mode is used so that the relay can communication with a UE in close proximity and we assume the relay is capable of rechargeable functionality. So the power consumed for relaying comes directly from electromagnetic waves, which can relieve the concern on limited battery life for typical IoT devices. With NOMA and relay, complete transmission cycle consists of two phases. In the first phase, the BS sends a composite signal to UE 1 and a selected relay device simultaneously by applying NOMA. After receiving the signal, the relay device splits the signal into two parts. One part is for information decoding and the other part is for energy harvesting. In the second phase, the BS sends another message to UE 1 while the relay device sends the decoded message to UE 2 by using the harvested energy in phase 1.

Denote the channel between BS and UE 1, BS and relay device, relay device and UE 2 as h'_{B1}, h'_{BR}, and h'_{R2}, respectively. Frequency flat quasi-static block fading model is used here so the channel does not change during the two transmission phases while the channel changes from cycle to cycle. Additionally, $h'_i = \frac{h_i\sqrt{a_0}}{\sqrt{1+d_i^\alpha}}$, where h_i is modeled as Rayleigh fading with $h_i \sim \mathcal{CN}(0,1), i = \{B1, BR, R2\}$[9]. a_0 is antenna-specific gain for the BS and $a_0 = 1$ when $i = R2$. An illustration of the system model is in Fig. 1.

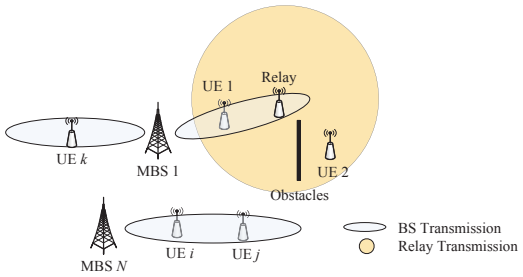

Fig. 1. System Model

In the following, the transmission process for each cycle is illustrated.

A. Phase 1 Transmission

In this phase, the BS sends the superimposed message to both UE 1 and the relay. The message is given as $x = \sqrt{\lambda_1 P_{BS}}x_1 + \sqrt{\lambda_2 P_{BS}}x_2$, where λ_1 and λ_2 are power allocation factors for UE 1 and the relay respectively with $\lambda_1 + \lambda_2 = 1$. x_1 and x_2 are normalized intended signal for UE 1 and UE 2. P_{BS} is the transmission power of the BS. At the receiver side, UE 1 observes y^1_{UE1}, which is expressed as

$$\begin{aligned} y^1_{UE1} &= \frac{h_{B1}\sqrt{a_0}}{\sqrt{1+d_{B1}^\alpha}}x + n_{B1} \\ &= \frac{h_{B1}\sqrt{a_0}}{\sqrt{1+d_{B1}^\alpha}}(\sqrt{\lambda_1 P_{BS}}x_1 + \sqrt{\lambda_2 P_{BS}}x_2) + n_{B1}, \end{aligned} \tag{1}$$

where n_{B1} is the additive Gaussian white noise (AWGN) with variance σ^2, d_{B1} is the distance from the BS to UE 1, α is the path loss exponent for line-of-sight (LOS).

Without loss of generality, we assume $|h_{B1}|^2 > |h_{BR}|^2$. Hence according to NOMA protocol, $\lambda_1 < \lambda_2$ is set to ensure QoS at the weak receiver. With this setting, UE 1 first decodes signal x_2 with its SINR formulated as

$$\gamma^1_{UE1,x_2} = \frac{\lambda_2 \rho_{B1}|h_{B1}|^2}{\lambda_1 \rho_{B1}|h_{B1}|^2 + 1}, \tag{2}$$

where $\rho_{B1} = \frac{P_{BS}a_0}{\sigma^2(1+d_{B1}^\alpha)}$ is the transmission SNR from the BS to UE 1. The superscript "1" indicates the first phase. SIC is performed to remove x_2 from the superimposed signal, then UE 1 can decode its own message with the following SINR

$$\gamma^1_{UE1,x_1} = \lambda_1 \rho_{B1}|h_{B1}|^2. \tag{3}$$

At the relay side, it first splits the observation into two parts. One part is for the rechargeable unit, which consists of a super capacitor or a short-term high efficiency battery. The other part is for information decoding, which can be expressed as

$$\begin{aligned} y^D_R &= \frac{h_{BR}\sqrt{a_0}}{\sqrt{1+d_{BR}^\alpha}}x\sqrt{1-\beta} + n_{BR} \\ &= \frac{h_{BR}\sqrt{a_0}}{\sqrt{1+d_{BR}^\alpha}}\sqrt{1-\beta}(\sqrt{\lambda_1 P_{BS}}x_1 + \sqrt{\lambda_2 P_{BS}}x_2) + n_{BR}, \end{aligned} \tag{4}$$

where β is the power split coefficient indicating the portion of power assigned to energy harvest unit. n_{BR} has the same

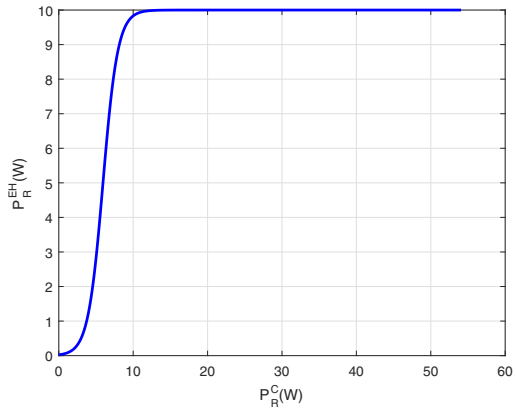

Fig. 2. Power-in-power-out response in the Non-Linear Energy Harvest Model

distribution with n_{B1}. Signal y_R^D goes through the decoding unit for x_2, the corresponding SINR is

$$\gamma_{R,x_2}^1 = \frac{(1-\beta)\lambda_2 \rho_{BR}|h_{BR}|^2}{(1-\beta)\lambda_1 \rho_{BR}|h_{BR}|^2 + 1}, \tag{5}$$

where $\rho_{BR} = \frac{P_{BS}a_0}{\sigma^2(1+d_{BR}^{\alpha})}$ is the transmission SNR from the BS to the relay.

The remaining power $P_R^C = |h_{BR}|^2 \beta \rho_{BR} \sigma^2$ is harvested by the relay. In this paper, we adopt the non-linear energy harvest model, which is more precise in modeling the power-in-power-out relation in current wireless charging technology. Specifically, the harvested energy can be expressed as a logistic (sigmoidal) function

$$P_R^{EH} = \frac{M}{1 + \exp\big(-a(P_R^C - b)\big)}, \tag{6}$$

where M, a, b are constants and represent different physical meanings in wireless charging. M denotes the maximum harvested power at the relay when the energy harvesting circuit is saturated. a together with b capture the joint effect of resistance, capacitance and circuit sensitivity [10].

[8] provides a more sophisticated model, which captures the zero-input-zero-output feature in wireless charging and can be modeled in the following.

$$P_R^{EH} = \frac{\Psi - M\Omega}{1-\Omega}, \quad \Omega = \frac{1}{1+\exp(ab)}, \tag{7}$$

where $\Psi = \frac{M}{1+\exp\big(-a(P_R^C - b)\big)}$.

In the subsequent analysis, we use model (6) based on the following reasons. 1) Our model does not have zero power input case; 2) The general logistic function can reduce the complexity in outage analysis; 3) (6) can provide sufficient precision.

Fig. 2 persents the power-in-power-out relation with 1000 independent events, based on which the parameters are estimated as follows, $\beta = 0.6$, $\sigma = 0.0995$, $M = 10$, $a = 1$, $b = \beta \rho_{BR} \sigma^2$, and $\rho_{BR} = 30$ dB.

B. Phase 2 Transmission

During the second phase, the relay sends x_2 to UE 2 with the energy harvested in *Phase 1*. Meanwhile, the BS sends another signal x_3 to UE 1. The received signal at UE 1 and UE 2 are expressed as

$$y_{UE1}^2 = \sqrt{P_{BS}} \frac{h_{B1}\sqrt{a_0}}{\sqrt{1+d_{B1}^{\alpha}}} x_3 + \sqrt{P_R^{EH}} \frac{h_{R1}}{\sqrt{1+d_{R1}^{\alpha}}} x_2 + n_{B1} \tag{8}$$

and

$$y_{UE2}^2 = \sqrt{P_R^{EH}} \frac{h_{R2}}{\sqrt{1+d_{R2}^{\alpha}}} x_2 + n_{B2}, \tag{9}$$

respectively.

Since UE 1 already decodes x_2 in *Phase 1*, by appropriately estimating the channel h_{R1}, it can employ SIC to subtract x_2 from its observation [11]. The remaining SINR becomes

$$\gamma_{UE1,x_3}^2 = \rho_{B1}|h_{B1}|^2. \tag{10}$$

For UE 2, since there is a severe blockage between BS and itself, it has a negligible interference from BS. The achievable SINR at UE 2 is

$$\gamma_{UE2.x_2}^2 = \rho_{EH}|h_{R2}|^2, \tag{11}$$

with $\rho_{EH} = \frac{P_R^{EH}}{\sigma^2(1+d_{R2}^{\alpha})}$.

III. Outage Analysis

In this section, we will provide mathematical analysis on the outage probability of the proposed scheme. The outage probability is defined as the probability of events where certain measurements such as SINR or data rate cannot meet the pre-defined threshold.

A. UE 1 Outage Probability

Define the minimum data rates for for messages x_1, x_2 and x_3 as R_1, R_2 and R_3 respectively. Below the minimum data rate, a UE will have an outage. Since UE 1 involves in both phases, outage occurs when UE 1 fails to decode x_2 and x_1 in phase 1 or fails to decode x_3 in phase 2. For simplicity, we can consider the complementary event first. Specifically, we can derive the outage probability of UE 1 as follows.

$$\begin{aligned} P(\mathcal{O}_{UE1}) &= 1 - P(\mathcal{O}_{UE1}^C) \\ &= 1 - P\bigg(\frac{1}{2}\log_2(1+\gamma_{UE1,x_2}^1) > R_2 \\ &\quad \& \ \frac{1}{2}\log_2(1+\gamma_{UE1,x_1}^1) > R_1 \\ &\quad \& \ \frac{1}{2}\log_2(1+\gamma_{UE1,x_3}^2) > R_3\bigg). \end{aligned} \tag{12}$$

Notice that channel $h_{B1} \sim \mathcal{CN}(0,1)$ and $|h_{B1}|^2 \sim \exp(1)$. Define $z_1 = 2^{2R_1} - 1$, $z_2 = 2^{2R_2} - 1$ and $z_3 = 2^{2R_3} - 1$.

$$\begin{aligned} P(\mathcal{O}_{UE1}) &= P(|h_{B1}|^2 > \phi_1) \\ &= 1 - e^{-\phi_1}, \end{aligned} \tag{13}$$

where $\phi_1 = \max\{\frac{z_2}{\lambda_2\rho_{B1} - z_2\lambda_1\rho_{B1}}, \frac{z_1}{\lambda_1\rho_{B1}}, \frac{z_3}{\rho_{B1}}\}$.

Note that the above outage probability is conditioned on $\lambda_2 > z_2\lambda_1$. Otherwise the outage occurs with probability 1.

B. UE 2 Outage Probability

For UE 2, since the BS only transmits x_2 via the relay. Thus the bottleneck of this transmission depends on the minimum data rate in two phases. The outage probability for UE 2 is

$$\begin{aligned} P(\mathcal{O}_{UE2}) &= 1 - P(\mathcal{O}_{UE2}^C) \\ &= 1 - P\bigg(\min\{\frac{1}{2}\log(1+\gamma_{R,x_2}^1), \\ &\quad \frac{1}{2}\log(1+\gamma_{UE2,x_2}^2)\} > R_2\bigg) \\ &= 1 - P\bigg(\min\{\gamma_{R,x_2}^1, \gamma_{UE2,x_2}^2)\} > z_2\}\bigg). \end{aligned} \tag{14}$$

The following theorem provides an analytical result for the outage probability of UE 2.

Theorem 1. *The outage probability for UE 2 in the proposed non-linear energy harvest model is* $P(\mathcal{O}_{UE2}) = 1 - \frac{c_2}{c_4} e^{-c_1}(c_3 e^{-c_1 c_4})^{-\frac{1}{c_4}} \Gamma(\frac{1}{c_4}, c_3 e^{-c_1 c_4})$*, where* c_1, c_2, c_3 *and* c_4 *are constants and defined in the following proof.*

Proof: Let $c = (1 + d_{R2}^{\alpha})$, the outage probability becomes

$$\begin{aligned} P(\mathcal{O}_{UE2}) &= 1 - P(\min\{\gamma_{R,x_2}^1, \gamma_{UE2,x_2}^2\} > z_2) \\ &= 1 - P(\gamma_{R,x_2}^1 > z_2, \gamma_{UE2,x_2}^2 > z_2). \end{aligned} \tag{15}$$

Let probability $P(\gamma_{R,x_2}^1 > z_2, \gamma_{UE2,x_2}^2 > z_2)$ be P_1 for conciseness. Furthermore, let $|h_{BR}|^2 = x$ and $|h_{R2}|^2 = y$. x and y both follow an exponential distribution with parameter 1 and they are independent to each other.

$$\begin{aligned} P_1 &= P(\frac{(1-\beta)\lambda_2 \rho_{BR} x}{(1-\beta)\lambda_1 \rho_{BR} x + 1} > z_2, \frac{P_R^{EH}}{\sigma^2 c} y > z_2) \\ &\overset{a}{=} P(x > \frac{z_2}{(1-\beta)\rho_{BR}(\lambda_2 - \lambda_1 z_2)}, \\ &\quad \frac{M}{\sigma^2 c(1+\exp(-a(\beta\rho_{BR}\sigma^2 x - b)))} y > z_2), \end{aligned} \tag{16}$$

where $\overset{a}{=}$ is conditioned on $\lambda_2 > \lambda_1 z_2$. Otherwise the outage probability will be always equal to one, as already observed in the existing literature. Define $f(x) = \frac{M}{\sigma^2 c(1+\exp(-a(\beta\rho_{BR}\sigma^2 x - b)))}$ and let $c_1 = \frac{z_2}{(1-\beta)\rho_{BR}(\lambda_2 - \lambda_1 z_2)}$. The above joint probability can be evaluated as

$$\begin{aligned} P_1 &= \int_{c_1}^{\infty} \int_{\frac{z_2}{f(x)}}^{\infty} e^{-x} e^{-y} dx dy \\ &= \int_{c_1}^{\infty} \exp\big(-x - \frac{z_2}{f(x)}\big) dx. \\ &= e^{-\frac{z_2 \sigma^2 c}{M}} \int_{c_1}^{\infty} \exp\Big(-x - \frac{z_2 \sigma^2 c}{M} e^{ab} \exp(-a\beta\rho_{BR}\sigma^2 x)\Big) dx. \end{aligned} \tag{17}$$

For notation simplicity, define $c_2 = e^{-\frac{z_2\sigma^2 c}{M}}$, $c_3 = \frac{z_2\sigma^2 c}{M} e^{ab}$ and $c_4 = a\beta\rho_{BR}\sigma^2$. Then P_1 can be simplified as

$$P_1 = c_2 \int_{c_1}^{\infty} \exp(-c_3 e^{-c_4 x} - x) dx. \tag{18}$$

Let $u = xc_4 - c_1 c_4, u \in [0, \infty]$. According to ([12], 3.331-1)

$$\begin{aligned} P_1 &= \frac{c_2}{c_4} e^{-c_1} \int_0^{\infty} \exp(-c_3 e^{-c_1 c_4} e^{-u} - \frac{u}{c_4}) du \\ &= \frac{c_2}{c_4} e^{-c_1} (c_3 e^{-c_1 c_4})^{-\frac{1}{c_4}} \Gamma(\frac{1}{c_4}, c_3 e^{-c_1 c_4}). \end{aligned} \tag{19}$$

$\Gamma(\mu_2, \mu_1)$ is the lower incomplete gamma function, which is

$$\Gamma(\mu_2, \mu_1) = \int_0^{\mu_1} e^{-t} t^{\mu_2 - 1} dt, \tag{20}$$

where $\mu_2 > 0$.

■

C. Outage at High SNR

In this subsection, we provide the approximation for the outage probability at high SNR region. Specifically, if $\rho_{B1}, \rho_{BR} \to \infty$, the outage probability for UE 1 becomes

$$P(\mathcal{O}_{UE1}^H) = \phi_1 = \max\{\frac{z_2}{\lambda_2 \rho_{B1} - z_2 \lambda_1 \rho_{B1}}, \frac{z_1}{\lambda_1 \rho_{B1}}, \frac{z_3}{\rho_{B1}}\}, \tag{21}$$

since $\lim_{x \to 0}(1 - e^{-x}) \simeq x$.

For UE 2, the maximum charging power is M even when P_R^C becomes infinity. Thus, the high approximation becomes

$$P(\mathcal{O}_{UE2}^H) = 1 - P(\frac{\lambda_2}{\lambda_1} > z_2, \frac{M}{\sigma^2(1 + d_{R_2}^{\alpha})} |h_{R2}|^2 > z_2). \tag{22}$$

When $\frac{\lambda_2}{\lambda_1} > z_2$, the result becomes

$$P(\mathcal{O}_{UE2}^H) = 1 - e^{-\frac{z_2 \sigma^2 (1 + d_{R_2}^{\alpha})}{M}}. \tag{23}$$

Otherwise, if $\frac{\lambda_2}{\lambda_1} < z_2$, the outage probability will be always one in the high SNR regime.

D. Diversity Analysis for UE 2

Based on the definition of diversity, we have

$$d_{UE2} = -\lim_{\rho_{BR} \to \infty} \frac{\log P(\mathcal{O}_{UE2})}{\log \rho_{BR}} = 0. \tag{24}$$

This means in the non-linear energy harvest model, no diversity will be achieved. The reason is that as the input power increases, the power harvested becomes saturated, which limits the further data rate growth hence the outage probability performance.

IV. Numerical Performance Results

In this section, numerical performance results are presented based on both simulations and analysis. The parameters for evaluation are chosen in the following. $a_0 = 4$, which indicates the horn antenna gain is 6 dB. $\lambda_1 = 0.4$, $\lambda_2 = 0.6$. $M = 4$, which means the maximum charging power for the relay is 4 Watts. For illustration purposes, the distance d_{BR}, d_{R2} and d_{B1} are small, which are set to 8, 2, and 10, respectively. Similar settings can also be found in [6]. Furthermore, the predefined thresholds for data rates are $R1 = R3 = 0.5$ bps/Hz and $R2 = 0.3$ bps/Hz.

Fig. 3 shows the outage probability of UE 1 and UE 2 with regards of the transmission SNR in dB. "ana" stands

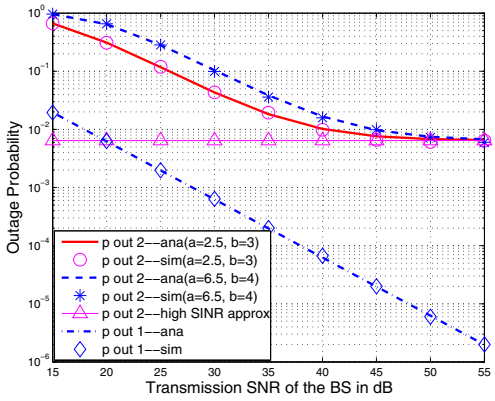

Fig. 3. Outage Performance for Both UEs with Comparison to Analytical Results

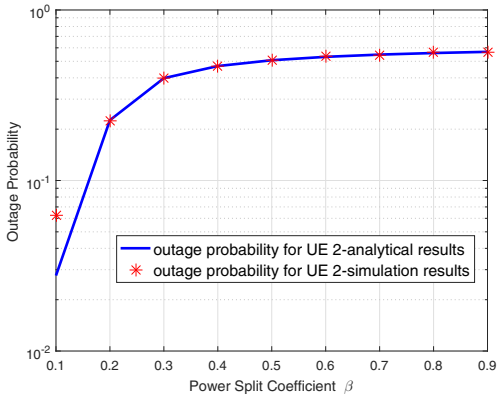

Fig. 4. Outage Performance for UE 2 as the Function of β

for analytical result while "sim" is the simulation one. The performance can be optimized by carefully choosing λ_1 and λ_2. The detailed study on how to select λ_1 and λ_2 values to achieve optimal performance is not the focus of this paper and hence not extended. Further, since a and b can also impact the system performance, the outage probability of UE 2 is evaluated with different a, b values. By fixing $\beta = 0.8$, both the simulation and analytical results are presented. As we can see from Fig. 3, the analytical results match well with the simulation ones for UE 1. As expected, the outage probability decreases linearly in log scale with the increase of transmission SNR. For UE 2, when $a = 2.5, b = 3$, the outage probability of UE 2 is lower than the case with $a = 6.5, b = 4$, which indicates that energy harvest circuit will affect the system performance. Also, as the transmission SNR becomes larger, the gap becomes less apparent. The reason is as SNR becomes larger, the harvested energy becomes a constant M, thus the outage performance becomes the same regarding different a and b values, as shown in the high SNR approximation part. Note that the non-linear response will only make sure the harvested energy does not exceed M. In some rare occasions, we can have $P_R^C < P_R^{EH}$, which clearly violates the physical meaning in our model. So these events are excluded from the results.

The outage performance for UE 2 as the function of β is shown in Fig. 4. The parameters used for this study are $a = 2, \rho_{BR} = 40$ dB. The simulation and analytical results for UE 2 are both presented here and they match well with each other. With the increase of β, the outage probability also increases. The increase slope slows down as β further increases, due to the fact that β is the portion of power assigned to energy harvest unit. The less power remained for transmitting, the higher outage probability it will have. The inconsistence between simulation and analytical results when $\beta = 0.1$ comes from the excluded events when $P_R^C < P_R^{EH}$.

V. Conclusions

In this paper, we consider applying NOMA and D2D relaying in a mmWave based wireless system that consists of high power base stations and low power IoT devices. The lower power IoT devices do not have external power supplies and have limited battery life. In order to prolong battery life and also to motivate low power IoT devices to help relay signals from others, low power IoT devices can harvest energy from electromagnetic signals. To make the energy harvest model more realistic, non-linear energy harvesting model is used. The theoretical analysis on outage probability is given for the proposed scheme and system model. Simulation results validate the accuracy of the analysis.

References

[1] R. Q. Hu and Y. Qian, "An Energy Efficient and Spectrum Efficient Wireless Heterogeneous Network Framework for 5G Systems," *IEEE Commun. Mag.*, vol. 52, no. 5, May 2014, pp. 94-101.

[2] Y. Saito, Y. Kishiyama, A. Benjebbour, T. Nakamura, A. Li, and K. Higuchi, "Non-orthogonal multiple access (NOMA) for future radio access," in *Proc. IEEE VTC spring 2013*, Jun. 2013.

[3] Y. Xu, H. Sun, R. Q. Hu, and Y. Qian, "Cooperative Nonorthogonal Multiple Access in Heterogeneous Networks," in *Proc. IEEE GlOBECOMM 2015*, San Diego, Dec. 2015.

[4] Z. Ding, Z. Yang, P. Fan, and H. V. Poor, "On the performance of nonorthogonal multiple access in 5G systems with randomly deployed users," *IEEE Signal Process. Lett.*, vol. 21, no. 12, pp. 1501-1505, Dec. 2014.

[5] P. Xu, Z. Ding, X. Dai and H. V. Poor, "NOMA: An Information Theoretic Perspective," *arXiv preprint arXiv:1504.07751*, 2015.

[6] Y. Liu, Z. Ding, M. Ekashlan and H. V. Poor, "Cooperative non-orthogonal multiple access in 5G systems with SWIPT," 2015 23rd European Signal Processing Conference (EUSIPCO), Nice, 2015, pp. 1999-2003.

[7] Y. Liu, Z. Ding, M. Elkashlan and H. V. Poor, "Cooperative Non-orthogonal Multiple Access With Simultaneous Wireless Information and Power Transfer," in *IEEE Journal on Selected Areas in Communications*, vol. 34, no. 4, pp. 938-953, April 2016.

[8] E. Boshkovska, R. Morsi, D. W. K. Ng and R. Schober, "Power allocation and scheduling for SWIPT systems with non-linear energy harvesting model," *2016 IEEE International Conference on Communications (ICC)*, Kuala Lumpur, 2016, pp. 1-6.

[9] Z. Ding, P. Fan, and H. V. Poor, "Random beamforming in millimeter-wave NOMA networks," *IEEE Trans. Commun.*, (submitted) Available on-line at arxiv.org/abs/1607.06302.

[10] E. Boshkovska, D. W. K. Ng, N. Zlatanov and R. Schober, "Practical Non-Linear Energy Harvesting Model and Resource Allocation for SWIPT Systems," in *IEEE Communications Letters*, vol. 19, no. 12, pp. 2082-2085, Dec. 2015.

[11] J.-B. Kim and I.-H. Lee, "Non-orthogonal multiple access in coordinated direct and relay transmission," *IEEE Commun. Lett.*, vol. 19, no. 11, pp. 2037?2040, Nov. 2015.

[12] I. S. Gradshteyn and I. M. Ryzhik, *Table of Integrals, Series, and Products.* Academic press, 2014.